Production and Identification of a Collisionless, Curvature-Driven, Trapped-Particle Instability

R. Scarmozzino, A. K. Sen, and G. A. Navratil
Plasma Physics Laboratory, Columbia University, New York, New York 10027
(Received 27 May 1986)

The Columbia Linear Machine has been redesigned to enter the parameter regime of the collisionless, curvature-driven, trapped-particle instability. With the new machine configuration, a strong ($\tilde{n}/N \gtrsim 60\%$), coherent mode is observed which bears all the characteristics of this instability. These include strong localization to the mirror cell, broad radial-mode structure, and MHD-like body motion of the plasma column. Furthermore, the mode exhibits all the correct parametric dependences of increasing mode amplitude with increasing mirror ratio and rf power, and decreasing mirror-cell length.

PACS numbers: 52.35.Py, 52.25.Gj

Trapped-particle instabilities have been the subject of considerable theoretical study for nearly two decades. Early theoretical studies[1-4] focused on trapped-particle instabilities in tokamaks and the associated anomalous transport. The direct experimental observation of these instabilities in tokamaks has been nearly impossible. This motivated the study of such dissipative instabilities[5-10] in the simpler geometry of the steady-state Columbia Linear Machine (CLM).[11] Recently[12,13] there has been considerable concern that a collisionless, curvature-driven, trapped-particle instability, with MHD-like growth rates, could arise in tandem mirrors. It is this instability which is currently being studied in the redesigned CLM (Fig. 1) and which we believe we have produced and identified. In contrast a collisional, curvature-driven, trapped-particle mode has recently been observed.[14]

To enter the parameter regime of the collisionless, curvature-driven, trapped-particle mode, we need to decrease the dissipative drive by reducing the collisionality below the previous value of $\nu_e/\omega^* \geq 0.03$, where ν_e is the electron Coulomb collision frequency and ω^* is the electron diamagnetic drift frequency. Furthermore, it is necessary to increase the curvature drive by raising the ion temperature and the trapped fraction above their previous values and operating with a shorter cell length. To obtain more quantitative information about the parameters needed for a strong collisionless mode, we solve the following trapped-particle mode dispersion relation[9]:

$$(1+\tau)-\delta\frac{4}{\sqrt{\pi}}\int_0^\infty dx\, x^2 \exp(-x^2)\frac{\omega-\omega^*[1+\eta_e(x^2-\frac{3}{2})]}{\omega-\omega_D x^2+i(\nu_e/\epsilon x^3+\nu_{en})} - \delta\tau\frac{4}{\sqrt{\pi}}\int_0^\infty dx\, x^2\exp(-x^2)\frac{\omega(1-b)+\omega^*/\tau}{\omega+\omega_D x^2/\tau+i(\nu_i/\epsilon x^3+\nu_{in})}=0. \quad (1)$$

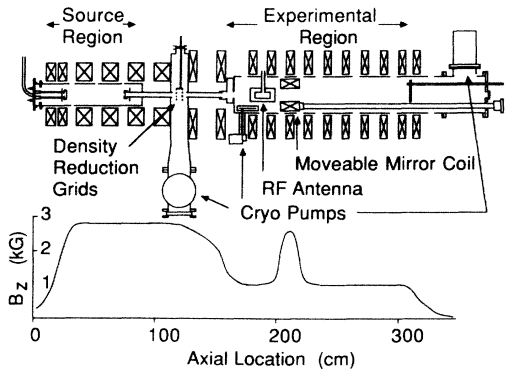

FIG. 1. Columbia Linear Machine.

This dispersion relation, which has been written for azimuthal mode number $m=1$, differs from that in Ref. 9 by the inclusion of ion finite Larmor radius (FLR). Here $x=v/v_{th}$, and ω, ω^*, ω_D, ν_j, and ν_{jn} are the complex mode frequency, electron diamagnetic drift frequency, electron curvature drift frequency, and Coulomb and neutral collision frequencies, respectively. The FLR parameter is $b=k_\perp^2\rho_i^2$, where $k_\perp$ is the transverse wave number and ρ_i is the ion Larmor radius. The trapped fraction is δ, $\tau=T_e/T_i$, $\eta_e=(N/N')/(T_e/T_e')$, $\epsilon=1-1/R_m$, and R_m is the mirror ratio. A numerical solution of this dispersion relation is shown in Fig. 2 for the following parameters: Case (A), $\omega^*=2.5\times10^5$ rad/sec, $\omega_D/\omega^*=0.005$, $\nu_{en}/\omega^*=0.015$, $\eta_e=1$, $\epsilon=0.67$, $b=0.02$, $\tau=1.3$, $\delta=60\%$; case (B), same as case (A), except $b=0.05$, $\tau=0.5$, $\delta=80\%$. This figure shows the growth rate and real

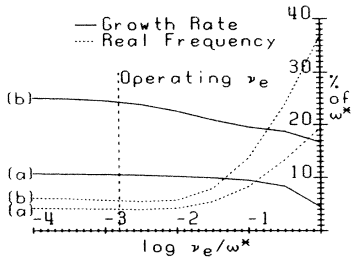

FIG. 2. Numerical solution of Eq. (1) for (a) case (A): $\omega^* = 2.5\times10^5$ rad/sec, $\omega_D/\omega^* = 0.005$, $\nu_e/\omega^* = 0.0015$, $\nu_{en}/\omega^* = 0.015$, $\eta_e = 1$, $\epsilon = 0.67$, $b = 0.02$, $\tau = 1.3$, $\delta = 60\%$; (b) case (B): same as case (A), except $b = 0.05$, $\tau = 0.5$, $\delta = 80\%$.

frequency of the mode versus the Coulomb collisionality. The graph indicates that if we reduce the collisionality to $\nu_e/\omega^* \sim 0.0015$, increase the curvature drive to $\omega_D/\omega^* \sim 0.005$, increase the ion temperature to obtain $b \sim 0.02$ to 0.05 and $\tau \sim 1.3$ to 0.5, and raise the trapped fraction to $\delta \sim 60\%$ to 80%, we can expect a strong mode with a growth rate of 10% to 25% of ω^*. The collisionless nature of the mode is apparent when we notice that the growth rate is much larger than the real frequency and that $\nu_e/|\omega| \sim 0.06 \ll 1$.

To achieve the necessary parameters, we have (i) improved the neutral pumping to reduce the neutral collisionality, (ii) inserted grids in the path of the plasma to lower the density and hence the Coulomb collisionality, (iii) installed an ion-cyclotron radio frequency heating system to raise the temperatures and the trapped fraction so as to further reduce the collisionality and increase the curvature drive. The rf heating system uses a slot-type antenna[15] driven at the ion-cyclotron frequency of 1.6 MHz and is capable of heating electrons as well as ions. Using this system we have obtained factor-of-2 improvements in electron and ion temperatures and in trapped fraction. With the present machine configuration (Fig. 1) we can achieve the following parameters: $T_e, T_i \sim 10$ eV, $N \sim 2\times10^8$ cm^{-3}, mirror cell length $L_c \sim 40$ cm, trapped fraction $\delta \sim 60\%$ to 80%. These experimental parameters are similar to those used in Fig. 2; therefore the CLM plasma is in the parameter range of the collisionless mode. Typical plasma-parameter radial profiles are shown in Fig. 3, and are measured with Langmuir and emissive probes and a gridded ion energy analyzer.

When the machine is configured as above, with high rf power and short cell length, a strong ($\tilde{n}/N \gtrsim 60\%$), coherent mode appears when the mirror is turned on. The real frequency of the mode is 70–80 kHz, and is much larger than the plasma frame frequency of ~ 2 kHz predicted by the above theory. However, a very crude estimate of the mode-averaged Doppler shift

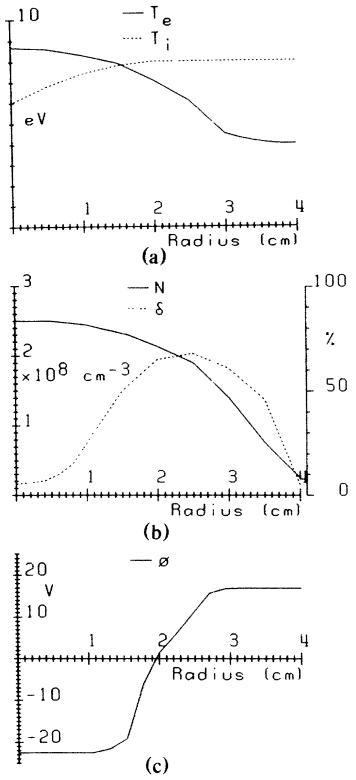

FIG. 3. Typical radial profiles of (a) electron and ion temperature, (b) plasma density and trapped fraction, and (c) plasma potential.

due to $\mathbf{E}\times\mathbf{B}$ rotation yields $\langle\omega_E\rangle/2\pi \sim 150$ kHz, which is within a factor of 2 of the observed frequency. The mode has an azimuthal mode number $m = 1$ and travels in the direction of $\mathbf{E}\times\mathbf{B}$ rotation. Numerical solution of the dispersion relation Eq. (1) indicates that $m = 2$ has a reduced growth rate and higher m modes are stabilized by FLR; therefore $m = 1$ is expected to be the dominant mode. The mode is flute-like in the mirror cell with $k_\parallel \sim 0$. The axial structure of the mode is shown in Fig. 4, along with a plot of the magnetic field. The mode is highly localized in the mirror cell, which is a fundamental characteristic of trapped-particle modes.

Various parametric dependences of the mode are displayed in Fig. 5. These figures show the frequency spectrum of density fluctuations sensed by a Langmuir probe biased to collect ion saturation current. We vary the mirror ratio, rf power, and mirror cell length about their nominal operating values of $R_m = 3.0$, $V_{rf} = 60$ V, $L_c = 45$ cm. Figure 5(a) shows the mode's dependence on mirror ratio R_m. At $R_m = 1.0$ there is a residual of the mode at 72 kHz, which we believe is an $\mathbf{E}\times\mathbf{B}$ rotationally driven mode. As R_m is increased this mode increases to 5 times its original amplitude, indicating that this mode is strongly driven by increasing mirror ratio. This parametric dependence on mir-

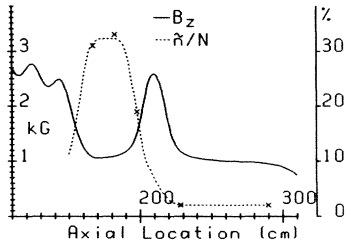

FIG. 4. Axial variation of mode amplitude shown along with the magnetic field. The dashed line is a sketch through the data points (crosses).

ror ratio is another identifying characteristic of trapped-particle modes. The mode's dependence on rf power is shown in Fig. 5(b). Here we see that with no rf heating the mode of interest, at 38 kHz, has a very small amplitude. As we increase the rf power the mode increases in amplitude and frequency. Increasing the rf power increases the temperatures and the trapped fraction and should therefore drive the instability more strongly, as observed. At $V_{rf}=60$ V the dc

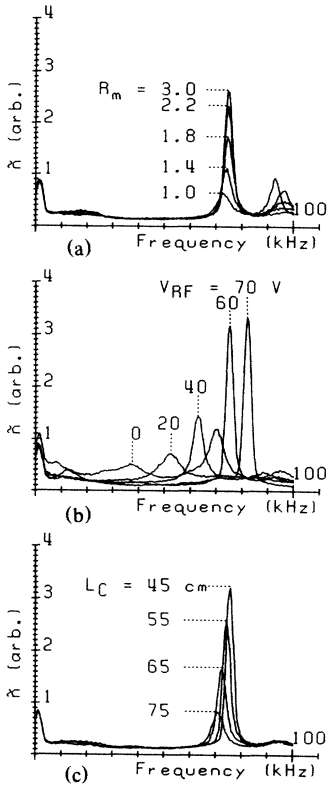

FIG. 5. Frequency spectrum of ion saturation-current fluctuations for varying (a) mirror ratio R_m, (b) rf voltage V_{rf}, and (c) mirror cell length L_c. In each case the other parameters are held constant at their nominal values of $R_m=3.0$, $V_{rf}=60$ V, $L_c=45$ cm.

electric field increases by about a factor of 2 as does the observed real frequency of the mode, supporting the statement that the real frequency of the mode is determined by some average Doppler shift $\langle\omega_E\rangle$. In Fig. 5(c) we show the mode's dependence on mirror cell length. For a long cell with $L_c=75$ cm, we see the mode at 72 kHz with small amplitude. As we reduce the cell length we see the mode being strongly driven. Decreasing the cell length from 75 to 45 cm increases the bounce-averaged magnetic curvature drive by about a factor of 2 and does not significantly change any other drive parameter; hence this parametric dependence directly demonstrates the curvature-driven nature of the mode. We have considered the possibility that the mode may be partially driven by $\mathbf{E}\times\mathbf{B}$ rotation. It is difficult to estimate its role because its contribution to the drive can vary widely depending on several effects: finite boundary, and passing and transit populations. We plan to make this difficult numerical calculation in the future.

The radial structure of the mode is very broad, with a half width at half maximum of the order of the density-gradient scale length. This is characteristic of a global, rigid mode, where the plasma column is moving as a whole. In contrast, the dissipative trapped-ion mode observed previously in this machine[8,9] was always highly localized around the position of maximum density gradient. To measure the "body motion" of the plasma, we have used a "stroboscopic" technique to measure the dynamic density profile $n(r,t)$. The technique uses the signal from one radially fixed Langmuir probe as a time reference to trigger the digitizers connected to two density-sensing Langmuir probes placed at equal radii but spaced 180° apart azimuthally. A complete measurement of $n(r,t)$ is obtained by our varying the radii of the two density-sensing probes. Figure 6 displays the density profile at two different times, one-half wave period apart, showing the plasma column displacement of over 1 cm from left to right in one-half wave period. This clear demonstration of the body motion of the plasma indicates a macroscopic MHD-like mode. Figure 7 shows the measured plas-

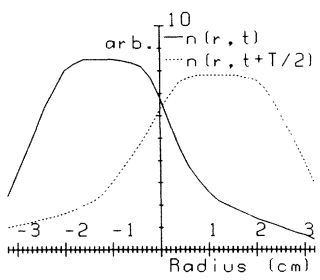

FIG. 6. Instantaneous ion saturation-current profiles at two times, $\frac{1}{2}$ wave period apart. T is one wave period.

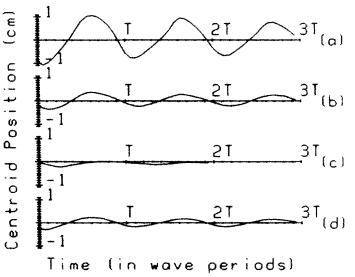

FIG. 7. Plasma centroid position vs time for various conditions of rf power and mirror cell length: (a) $V_{rf}=60$ V, $L_c=45$ cm; (b) $V_{rf}=45$ V, $L_c=45$ cm; (c) $V_{rf}=15$ V, $L_c=45$ cm; (d) $V_{rf}=60$ V, $L_c=75$ cm. The mirror ratio is held constant at $R_m=3.0$. T is one wave period.

ma centroid location versus time for various drive conditions. For low drive via low rf power or long cell length the centroid motion is less than a few millimeters as seen in Figs. 7(c) and 7(d). However, for high drive via high rf power and short cell length the centroid motion is largest at over 1 cm. This clearly indicates the correct parametric dependence of body motion on rf power and cell length for the curvature-driven trapped-particle mode.

In summary, we have produced a mode which has all the characteristics of a collisionless, curvature-driven, trapped-particle instability: strong localization in the mirror cell, broad radial structure, and macroscopic body motion of the plasma column. Furthermore, the mode exhibits all the correct parametric dependences: increasing fluctuation amplitude and plasma centroid motion with increasing mirror ratio, increasing rf power, and decreasing cell length. Hence, we believe that we have experimentally produced and definitively identified a collisionless, curvature-driven, trapped-particle mode. It is noted that a stabilization scheme based on having a sufficient passing population has been proposed.[12,13] Tandem mirrors are now designed to incorporate this idea.

This work was supported by U. S. Department of Energy Grant No. DE-FG02-84ER53182. Fruitful discussions with E. B. Hooper are gratefully acknowledged.

[1]B. B. Kadomtsev and O. P. Pogutse, Zh. Eksp. Teor. Fiz. **51**, 1734 (1966) [Sov. Phys. JETP **24**, 1172 (1967)].

[2]B. B. Kadomtsev and O. P. Pogutse, Nucl. Fusion **11**, 67 (1971).

[3]O. P. Pogutse, Nucl. Fusion **9**, 157 (1969).

[4]M. N. Rosenbluth, D. W. Ross, and D. P. Kostomarov, Nucl. Fusion **12**, 3 (1972).

[5]S. C. Prager, T. C. Marshall, and A. K. Sen, Plasma Phys. **17**, 785 (1975).

[6]D. P. Dixon, T. C. Marshall, and A. K. Sen, Plasma Phys. **20**, 189 (1978).

[7]D. P. Dixon, A. K. Sen, and T. C. Marshall, Plasma Phys. **20**, 225 (1978).

[8]J. Slough, G. A. Navratil, and A. K. Sen, Phys. Rev. Lett. **47**, 1057 (1981).

[9]G. A. Navratil, A. K. Sen, and J. Slough, Phys. Fluids **26**, 1044 (1983).

[10]A. B. Plaut, Ph.D. thesis, Columbia University, 1986 (unpublished).

[11]G. A. Navratil, J. Slough, and A. K. Sen, Plasma Phys. **24**, 185 (1982).

[12]D. E. Baldwin, Lawrence Livermore National Laboratory Report No. UCID-19359, 1982 (unpublished).

[13]H. L. Berk, M. N. Rosenbluth, H. V. Wong, T. M. Antonsen, and D. E. Baldwin, Fiz. Plazmy **9**, 176 (1983) [Sov. J. Plasma Phys. **9**, 108 (1983)].

[14]J. C. Fernandez, C. P. Chang, A. J. Lichtenberg, M. A. Lieberman, and H. Meuth, Phys. Fluids **29**, 1208 (1986).

[15]O. M. Shvets *et al.*, Fiz. Plazmy **7**, 485 (1981) [Sov. J. Plasma Phys. **7**, 261 (1981)].